Measurement and Calculation of Solubilities in the Ternary System $NaCH_3COO$ + NaCl + H_2O from 278 K to 323 K

Joachim Dorn and Michael Steiger*

Department of Chemistry, University of Hamburg, Martin-Luther-King-Platz 6, 20146 Hamburg, Germany

Solubility determinations in the ternary system $NaCH_3COO$ + NaCl + H_2O were performed from 278.15 K to 323.15 K. The new measurements were combined with previous measurements of osmotic coefficients at 298.15 K and activity coefficients from 298.15 K to 318.15 K. The measurements were fitted with an extended Pitzer type model to generate equations for the prediction of solubilities and activities in mixed solutions of the ternary system. The model yields accurate representation of the experimental data. Although it was found that the values of the mixing parameters in the ion interaction equations are significantly different from zero, their influence is only small. Hence, extrapolation to temperatures outside of the fitted range appears to be possible. However, due to limitations of the binary model equations for NaCl (aq) and $NaCH_3COO$ (aq) there is an upper ionic strength limit of about (15 to 18) $mol{\cdot}kg^{-1}$. Hence, solubility calculations are limited to temperatures below about 328 K.

Introduction

Salt crystallization in porous building materials not only limits the durability of the world's architectural heritage but is also a major cause of damage in porous museum artifacts. Damage is caused by the growth of salt crystals in the porous structures of materials such as stone or ceramics.[1] Acetate salts are frequently observed in efflorescences on calcareous objects in museum cabinets.[2−4] The formation of these salts is ultimately caused by emissions of acetic acid from the materials used for the construction of display cases.[5] Together with inorganic salts, for example, chlorides, nitrates, and sulfates, which are commonly present in porous materials, acetates form complex mixed electrolyte systems.[6] Similarly, mixed electrolyte solutions containing acetates and inorganic salts are also important in various industrial and laboratory processes, for example the Bayer process.[7]

The prediction of solubilities and crystallization behavior of such complex multicomponent electrolyte mixtures is an issue of major concern in these research areas. The prediction of phase equilibria requires the ability to calculate activity coefficients and water activities in mixed electrolyte solutions. One approach that has been successfully applied to the calculation of solubility equilibria is the ion interaction model of Pitzer.[8] The ion interaction equations contain empirical parameters that have to be determined from experimental data of binary and simple ternary mixtures. A search of the published literature revealed that there are substantial gaps in the available thermodynamic database.[9] Only few data are available for electrolyte mixtures containing inorganic salts and acetate or other organic anions.

The measurements reported here form part of an investigation of the thermodynamic properties of aqueous acetate and formate solutions and their mixtures with common inorganic salts. In a previous paper,[10] we reported on vapor pressure measurements of $NaCH_3COO$ + H_2O and determined the ion interaction parameters for this binary system. In the present work, we extend this treatment and provide new solubility data for ternary system $NaCH_3COO$ + NaCl + H_2O at near ambient temperatures. These data are used together with published thermodynamic data to determine the ternary interaction parameters that are required for the calculation of solubilities in more complex mixtures.

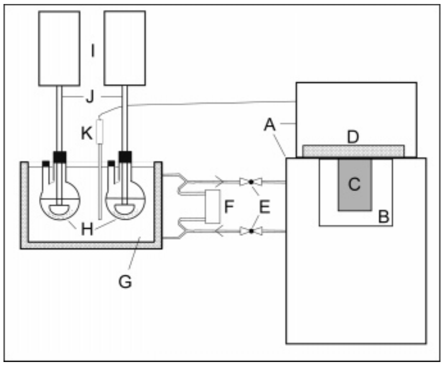

Figure 1. Schematic diagram of the solubility device: A, thermostat; B, internal bath (ca. 4 L); C, beaker; D, insulation; E, valves; F, insulated copper tube; G, external bath (ca. 6 L); H, round-bottom flaks with saturated solutions; I, KPG stirrers; J stirrer shafts; and K, Pt-100 resistance thermometer.

Experimental Section

Preparation of Saturated Solutions. Solubility measurements in the binary system $NaCH_3COO$ + H_2O were carried out in the range from 278.15 K to 333.15 K. Solubility isotherms in the ternary system $NaCH_3COO$ + NaCl + H_2O were determined at 278.15 K, 298.15 K, and 323.15 K. Solutions were prepared using anhydrous $NaCH_3COO$ and NaCl (analytical grade, Merck, Germany) without further purification and ultrapure water (resistivity of 18 MΩ·cm) supplied from a Seralpur pro 90c water purification system (Seral, Hamburg, Germany) and were filtered through a 0.2 μm membrane filter. A schematic diagram of the device used for the preparation of the saturated solutions is shown in Figure 1. Solutions were prepared by weighing the components into 250 mL flasks thermostated in an external water bath connected to a thermostat F25-MH (Julabo, Selbach, Germany). To avoid supersaturation, the amount of water added was such that there was always a solid residue. Water was added slowly to ensure that the temperature

---

* Corresponding author. Email: michael.steiger@chemie.uni-hamburg.de. Phone: +49 40 42838 2895. Fax: +49 40 42838 2893.

10.1021/je7001495 CCC: $37.00

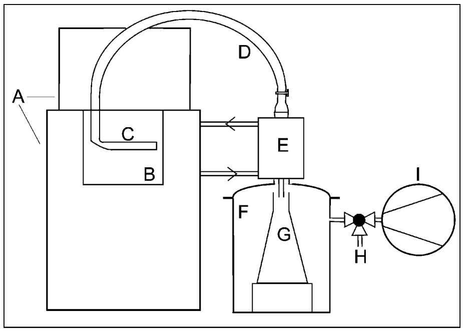

Figure 2. Schematic diagram of the solubility device: A, thermostat; B, internal bath (ca. 5 L); C, twisted tube humidifier; D, insulated hose; E, insulated copper tube; F, vacuum filtration device; G, flask; H, three-way valve; and I, membrane pump.

control could compensate for heat of solution effects. For equilibration, the suspensions were continuously stirred in the round-bottom flasks for one week. Inflow and outflow ports for the thermostated water were placed on opposite corners of the external bath resulting in a homogeneous temperature distribution (± 0.02 K). The external bath and the tubing were carefully insulated and the temperature difference between the external and the internal bath did not exceed 0.5 K for 278 K $< T <$ 333 K. The Pt-100 resistance thermometer used for temperature control in the external bath was calibrated using a mercury thermometer (Amarell, Kreuzwertheim, Germany) traceable to national standards.

Sampling of Saturated Solutions. Samples were taken from the saturated solutions using a cannula (0.8 mm × 120 mm, Sterican, Melsungen, Germany) connected to a syringe (Becton Dickinson, Basel, Switzerland). Cellulose nitrate membrane filters (5 μm) were used for the filtration of the samples (Schleicher & Schüll, Dassel, Germany). Cannula, syringes, and filter holders were thermostated overnight in an insulated copper tube (16 mm × 82 mm, see Figure 1). One hour before taking samples, stirring was interrupted to allow for the settlement of the suspension. The solution was withdrawn to the syringe using the cannula fed through a septum on the side neck of the flask. Approximately equal amounts of the sample were then weighed into two 50 mL volumetric flasks. The mass of water in the samples was determined by the difference of the total mass of the sample and the mass of the dissolved solutes as subsequently analyzed. The volumetric flasks were filled to the mark, and the solutions were stored in 30 mL polypropylene vessels at 253 K until they were analyzed. The first sample was drawn after 24 h followed by another three samples during the following 6 days. Sampling was carried out in duplicate.

Sampling of Wet Residue. To avoid any phase transformations in the wet residues during sample manipulation and analysis, care was taken to carry out the separation of solid and liquid phases and the solid-phase characterization under controlled conditions of temperature and relative humidity (RH). After the sampling of the saturated solutions, a capacitive humidity sensor (Hygrotec H1307, Titisee-Neustadt, Germany) was inserted through the side neck of the flask to measure the equilibrium humidity over the saturated solutions after an equilibration time of (2 to 3) h. Subsequently, suspensions were rapidly transferred to the filtration device schematically shown in Figure 2. The wet residue samples were obtained by decanting most of the saturated liquid phase into a twisted glass tube thermostated in the internal bath of a thermostat (RCS 6, Lauda, Germany) and were then filtered through a glass filter frit using a vacuum filtration device (Figure 2). During the filtration the glass tube with the filter frit was thermostated in an insulated copper tube (25 mm × 70 mm). To control the RH during the filtration, an airflow equilibrated with the saturated solution in the twisted glass tube humidifier was continuously drawn through the filtration device. Thus, filtration under constant isothermal conditions was ensured and the RH of the air during the filtration was equal to the equilibrium humidity of the saturated solution in the humidifier. After filtration, the solid samples were transferred into 13 mL polypropylene vessels and were then stored at the desired temperature until they were analyzed.

Analysis. Acetate and chloride in the saturated solutions were determined by potentiometric titration with a Titroprocessor 686 (Metrohm, Herisau, Switzerland). Acetate was determined by acidimetric titration with 0.05 mol·L^{-1} H_2SO_4. Chloride was determined by argentometric titration with 0.01 mol·L^{-1} $AgNO_3$. In a few samples, acetate was analyzed using ion chromatography. The chromatographic system consisted of an isocratic pump P 1000 (Thermo Separation Products, San Jose, CA), an automated sampler BT 7041 (Biotronik/Eppendorf, Hamburg, Germany), and an ion chromatograph 2000i with conductivity detector CDM−I (Dionex, Sunnyvale, CA). An ASRS-Ultra suppressor with SRS controller (Dionex) in the autosuppression recycle mode was employed for electrochemical suppression. Separation of the anions was achieved using a guard column AG 10 and a separation column AS 10 (Dionex) using a 100 mmol·L^{-1} NaOH eluent (analytical grade, Merck) at a flow rate of 1.2 mL·min^{-1}. As a further check of the anion determinations, the concentrations of the counterion sodium were measured in the saturated solutions using an inductively coupled plasma optical emission spectrometer (Plasma 2000, Perkin-Elmer, Überlingen, Germany). All determinations in the saturated solution were carried out in duplicate.

Wet residues were characterized by X-ray diffractometry (XRD) using a Siemens D5000 Bragg−Brentano parafocusing powder diffractometer with a vertical θ:2θ configuration using Cu Kα radiation and a position-sensitive detector (PSD) recording data from a 12° 2θ band at one time. The goniometer is equipped with a specially designed environmental cell[11] allowing for measurements to be made under controlled conditions of temperature and RH (RH-XRD). XRD measurements were carried out at the temperature of the solubility measurements and at the equilibrium RH of the respective saturated solutions.

Equations

In the Pitzer approach,[8] the osmotic coefficient for a single 1−1 electrolyte MX is given by

$$(\phi - 1) = f^{\phi} + m/m^{\circ}B^{\phi}_{MX} + m^2/m^{\circ 2}C^{\phi}_{MX} \qquad (1)$$

where m is the molality, m° denotes the unit molality of 1 mol·kg^{-1}, and f^{ϕ}, the Debye−Hückel long-range electrostatic term, is given by

$$f^{\phi} = -A_{\phi}I^{1/2}/(1 + bI^{1/2}) \qquad (2)$$

where A_{ϕ} is the Debye−Hückel parameter for the osmotic coefficient whose values at the studied temperatures were taken from Archer and Wang,[12] b is a constant ($b = 1.2$ kg$^{1/2}$·mol$^{-1/2}$), and I is the ionic strength, which for a single 1−1 electrolyte is equivalent to the molality. B^{ϕ}_{MX} and C^{ϕ}_{MX} are the second and third virial coefficients in the ion interaction approach. B^{ϕ}_{MX} depends on the ionic strength

$$B^{\phi}_{MX} = \beta^{(0)}_{MX} + \beta^{(1)}_{MX}\exp(-\alpha_1 I^{1/2}) + \beta^{(2)}_{MX}\exp(-\alpha_2 I^{1/2}) \qquad (3)$$

where the interaction parameters $\beta^{(0)}_{MX}$, $\beta^{(1)}_{MX}$, $\beta^{(2)}_{MX}$, and C^{ϕ}_{MX} are specific to the salt MX, and α_1 and α_2 are numerical constants. The mean activity coefficient γ_{MX} of a single salt solution in the ion interaction approach is given by

$$\ln \gamma_{MX} = f^{\gamma} + m/m^{\circ}\, B^{\gamma}_{MX} + m^2/m^{\circ 2} C^{\gamma}_{MX} \tag{4}$$

and the Debye–Hückel term f^{γ} for the activity coefficient is given by

$$f^{\gamma} = -A_{\phi}[I^{1/2}/(1 + bI^{1/2}) + 2/b \ln(1 + bI^{1/2})] \tag{5}$$

The function B^{γ}_{MX} is defined as

$$B^{\gamma}_{MX} = B_{MX} + B^{\phi}_{MX} \tag{6}$$

with

$$B_{MX} = \beta^{(0)}_{MX} + (2\beta^{(1)}_{MX}/\alpha_1{}^2 I)[1 - (1 + \alpha_1 I^{1/2}) \exp(-\alpha_1 I^{1/2})] + (2\beta^{(2)}_{MX}/\alpha_2{}^2 I)[1 - (1 + \alpha_2 I^{1/2}) \exp(-\alpha_2 I^{1/2})] \tag{7}$$

Also

$$C^{\gamma}_{MX} = 3/2 C^{\phi}_{MX} \tag{8}$$

The ion interaction parameters $\beta^{(0)}_{MX}$, $\beta^{(1)}_{MX}$, $\beta^{(2)}_{MX}$, and C^{ϕ}_{MX} have to be determined from single electrolyte experimental data. Originally, the $\beta^{(2)}_{MX}$ term in eqs 3 and 6 was introduced for the treatment of the bivalent metal sulfates to avoid the explicit calculation of association equilibria.[13] Later, it was found that the numerical flexibility at very high concentrations is enhanced by inclusion of the $\beta^{(2)}_{MX}$ term together with appropriate values of α_2.[14] This approach was successfully applied in our previous work[1,10] to represent the thermodynamic properties of various electrolytes to high ionic strength.

For a mixture of two 1–1 electrolytes with a common cation M, the expression for the osmotic coefficient is

$$(\phi - 1) = f^{\phi} + m/m^{\circ}[(1 - y)B^{\phi}_{MX} + yB^{\phi}_{MY}] + m^2/m^{\circ 2}[(1 - y)C^{\phi}_{MX} + yC^{\phi}_{MY}] + y(1 - y)m/m^{\circ}(\theta_{XY} + m/m^{\circ}\psi_{MXY}) \tag{9}$$

where m is the total molality, y is the solute fraction of the component MY, and θ_{XY} and ψ_{MXY} are the mixing parameters. The activity coefficient of MX in the ternary mixture is

$$\ln\gamma_{MX} = f^{\gamma} + m/m^{\circ}[B_{MX} + (1 - y)B^{\phi}_{MX} + yB^{\phi}_{MY}] + m^2/m^{\circ 2}[(3/2 - y)C^{\phi}_{MX} + yC^{\phi}_{MY}] + ym/m^{\circ}[\theta_{XY} + (1 - y/2)m/m^{\circ}\psi_{MXY}] \tag{10}$$

Using eqs 9 and 10, the mixing parameters are determined from experimental osmotic and activity coefficients of the common cation ternary mixtures by calculating the differences between experimental values and values calculated with all binary interaction parameters. The differences between experimental and calculated values can be expressed in terms of the mixing parameters that can then be calculated.[8]

The standard solubility product K_{MX} of a hydrated solid $MX \cdot \nu_0 H_2O$ of a 1–1 electrolyte is given by

$$\ln K_{MX} = \ln(m_M/m^{\circ}) + \ln(m_M/m^{\circ}) + 2 \ln \gamma_{MX} + \nu_0 \ln a_w \tag{11}$$

where m_M, m_X, and $\ln \gamma_{MX}$ refer to the saturated solution of the salt. The water activity a_w is related to the osmotic oefficient

$$\ln a_w = -2\phi M_w m \tag{12}$$

Here, $M_w = 0.0180153$ kg·mol^{-1} is the molecular mass of water. If the values of the equilibrium constants are known, experimental solubility data can be used to determine the mixing parameters by calculating the activity products for the saturated solution molalities with the appropriate binary interaction parameters. The deviations of these activity products from the thermodynamic equilibrium constants can then be used to obtain the mixing parameters.

Table 1. Molal Solubilities in the System $NaCH_3COO + H_2O$

T/K	m/mol·kg^{-1}	solid phase
278.15	4.74 ± 0.06	$NaCH_3COO \cdot 3H_2O$
298.15	6.21 ± 0.04	$NaCH_3COO \cdot 3H_2O$
313.15	7.71 ± 0.08	$NaCH_3COO \cdot 3H_2O$
323.15	10.7 ± 0.1	$NaCH_3COO \cdot 3H_2O$
328.15	12.5 ± 0.2	$NaCH_3COO \cdot 3H_2O$
333.15	17.0 ± 0.4	$NaCH_3COO$

Table 2. Molal Solubilities in the System $NaCH_3COO + NaCl + H_2O$

$m(NaCH_3COO)$ mol·kg^{-1}	$m(NaCl)$ mol·kg^{-1}	solid phases
	T = 278.15 K	
1.02 ± 0.01	5.37 ± 0.06	NaCl
2.05 ± 0.01	4.61 ± 0.05	NaCl
3.10 ± 0.01	3.88 ± 0.03	$NaCH_3COO \cdot 3H_2O$ + NaCl
3.11 ± 0.01	3.91 ± 0.05	$NaCH_3COO \cdot 3H_2O$ + NaCl
3.10 ± 0.02	3.89 ± 0.04	$NaCH_3COO \cdot 3H_2O$ + NaCl
3.81 ± 0.01	2.03 ± 0.02	$NaCH_3COO \cdot 3H_2O$
3.71 ± 0.03	2.26 ± 0.01	$NaCH_3COO \cdot 3H_2O$
4.26 ± 0.02	1.03 ± 0.01	$NaCH_3COO \cdot 3H_2O$
	T = 298.15 K	
1.02 ± 0.01	5.47 ± 0.07	NaCl
2.02 ± 0.01	4.69 ± 0.05	NaCl
3.01 ± 0.06	4.00 ± 0.10	NaCl
4.67 ± 0.04	3.15 ± 0.03	NaCl
4.93 ± 0.02	2.99 ± 0.04	$NaCH_3COO \cdot 3H_2O$ + NaCl
4.95 ± 0.02	2.98 ± 0.01	$NaCH_3COO \cdot 3H_2O$ + NaCl
5.14 ± 0.02	2.47 ± 0.01	$NaCH_3COO \cdot 3H_2O$
5.96 ± 0.02	0.644 ± 0.008	$NaCH_3COO \cdot 3H_2O$
	T = 323.15 K	
1.01 ± 0.01	5.73 ± 0.11	NaCl
2.05 ± 0.01	5.07 ± 0.12	NaCl
3.07 ± 0.03	4.33 ± 0.08	NaCl
5.07 ± 0.03	3.24 ± 0.07	NaCl
7.16 ± 0.06	2.38 ± 0.02	NaCl
10.01 ± 0.08	1.54 ± 0.01	$NaCH_3COO \cdot 3H_2O$ + NaCl
9.92 ± 0.08	1.55 ± 0.01	$NaCH_3COO \cdot 3H_2O$ + NaCl
10.12 ± 0.07	0.774 ± 0.005	$NaCH_3COO \cdot 3H_2O$

Results and Discussion

Solubility Measurements. The present solubility measurements are summarized in Table 1 for the binary system $NaCH_3COO + H_2O$ and in Table 2 for the ternary system $NaCH_3COO + NaCl + H_2O$, respectively. The values listed are average values of eight replicates, that is, four sets of duplicate measurements. The uncertainties given are the standard deviations of these determinations. All solid phases could be unambiguously identified using RH-XRD by comparison with JCPDS-ICDD standards 28–1030 ($NaCH_3COO \cdot 3H_2O$), 28–1029 ($NaCH_3COO$), and 05–1028 (NaCl). Our solubilities in the binary system are in good agreement with available literature data[15–20] (Figure 3). In agreement with the transition temperature of 331.15 K for the dehydration of sodium acetate trihydrate reported in the literature,[21] we found the anhydrous salt as the stable solid at 333.15 K and the trihydrate at 328.15 K and below. No data are available in the literature for the ternary system at the temperatures studied.

Binary Model Parameters. Beyer and Steiger[10] reported a comprehensive evaluation of the thermodynamic properties of aqueous $NaCH_3COO$ and were able to represent accurately these

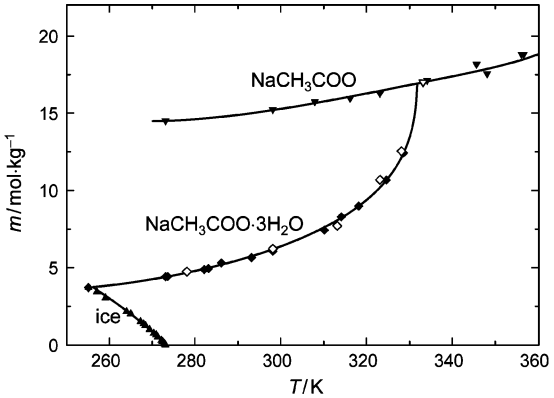

Figure 3. Experimental and calculated (—) freezing temperatures and solubilities in the system $NaCH_3COO + H_2O$. Symbols refer to experimental freezing temperatures[15,22,23] (▲) and solubilities[15−20] of $NaCH_3COO·3H_2O$ (◆,◇) and $NaCH_3COO$ (▼,▽); open symbols represent the measurements of the present work.

Table 3. Parameters of Equation 13 for $NaCH_3COO$(aq) and NaCl(aq)

$P(T)$		$NaCH_3COO$[a]	NaCl
$\beta^{(0)}$	q_1	1.73520E −01	2.56901E −01
	q_2		
	q_3	−5.78873E −01	−4.92791E −01
$\beta^{(1)}$	q_1	1.07355E +01	5.65743E −01
	q_2	−3.01478E +04	−3.35868E +02
	q_3	−1.59618E +02	−1.87839E +00
	q_4	2.26150E −01	
	q_5		
	q_6	−2.42496E +00	
$\beta^{(2)}$	q_1	−4.58763E +00	−1.09130E +00
	q_2		
	q_3	−4.93400E +01	9.01392E −01
	q_4	2.68732E −01	
	q_5	−1.89747E −04	
	q_6	1.04252E +00	1.48907E −01
C^{ϕ}	q_1	−6.99505E −03	−9.45386E −03
	q_2	7.48747E +00	
	q_3	4.41329E −02	1.77084E −02

[a] From Beyer and Steiger.[10]

data using the extended equation with both the $\beta^{(1)}_{MX}$ and the $\beta^{(2)}_{MX}$ term and values of 1.4 kg$^{1/2}$·mol$^{-1/2}$ and 0.5 kg$^{1/2}$·mol$^{-1/2}$ for α_1 and α_2, respectively. They adopted the following temperature-dependent expression $P(T)$ for each parameter $\beta^{(0)}_{MX}$, $\beta^{(1)}_{MX}$, $\beta^{(2)}_{MX}$, and C^{ϕ}_{MX}:

$$P(T) = q_1 + q_2(1/T - 1/T_R)T^\circ + q_3 \ln(T/T_R) + q_4(T - T_R)/T^\circ + q_5(T^2 - T_R{}^2)/T^{\circ 2} + q_6 \ln(T/T^\circ - 225) \quad (13)$$

with $T_R = 298.15$ K and $T^\circ = 1$ K. For convenience, the coefficients q_i for $NaCH_3COO$ (aq) taken from Beyer and Steiger are listed in Table 3. The number of digits given for all ion interaction parameters used in this work is sufficient to reproduce the calculations to about 0.0001 in ϕ and ln γ.

Though some osmotic coefficients from boiling temperatures that were used in the treatment of Beyer and Steiger[10] extend to 25 mol·kg^{-1}, the experimental data at lower temperatures are limited to maximum molalities of 15 mol·kg^{-1}. Test calculations have shown that the extrapolation to higher concentrations is critical. Calculated water activities show a minimum at molalities near 18 mol·kg^{-1} and the $NaCH_3COO$ activity runs through a broad maximum at around the same molality. This unrealistic behavior indicates that the equation should not be used above about (15 to 18) mol·kg^{-1}. This is not a severe restriction at the lower temperatures where the trihydrate is the stable solid. Thus, the available solubilities of $NaCH_3COO·3H_2O$ (see Figure 3) were used together with the model parameters for $NaCH_3COO$ (aq) listed in Table 3 to calculate values of the thermodynamic solubility product of the trihydrate from eq 11. These values of ln K were then fitted to eq 13 to represent the temperature dependence of the solubility product. The fitting constants for $NaCH_3COO·3H_2O$ are listed in Table 4 and the calculated solubilities are depicted in Figure 3. The number of digits given in Table 3 is sufficient to reproduce the solubility calculations to within 0.001 mol·kg^{-1}. The model represents the experimental solubilities to within the expected experimental uncertainties. The freezing temperature data[15,22,23] shown in Figure 3 are the same values that were used by Beyer and Steiger[10] in their treatment of $NaCH_3COO$ (aq). The calculated invariant point $NaCH_3COO·3H_2O$ + ice + solution at 256.17 K and $m = 3.74$ mol·kg^{-1} is in reasonable agreement with the very old values reported by Guthrie,[15] that is, 255.15 K and $m = 3.70$ mol·kg^{-1}.

Table 4. Coefficients in Equation 13 for the Temperature Dependence of the Solubility Products ln *K* of $NaCH_3COO·3H_2O$, $NaCH_3COO$, NaCl, and $NaCl·2H_2O$

	$NaCH_3COO·3H_2O$	$NaCH_3COO$	NaCl	$NaCl·2H_2O$
q_1	3.5536E +00	−2.06941E +01	−3.1947E -01	3.82650E +00
q_2				
q_3	8.4622E +00	−3.26335E +02	4.0577E +00	5.79886E +02
q_4		1.70167E +00	−2.0856E −02	−4.16737E +00
q_5		−1.20472E −03		3.80565E −03
q_6		6.56788E +00	9.2439E −01	

Despite of the problems expected at higher molalities, we have also used the model to determine the solubility product of anhydrous $NaCH_3COO$; the fitting constants of eq 13 are listed in Table 4, and the calculated solubilities in Figure 3 are in good agreement with the experimental data. The calculated transition temperature of 331.8 K agrees reasonably with the literature value[21] of 331.15 K and reflects the scatter in the solubility data. Although the model accurately represents the solubilities to 360 K, severe problems may occur if the model is applied to solubility calculations for anhydrous $NaCH_3COO$ in mixed systems at enhanced temperature where the saturated solutions exhibit even higher ionic strengths. Test calculations not presented here have shown that these problems at very high ionic strength can be overcome with modified binary interaction parameters for $NaCH_3COO$ (aq) such that a more realistic behavior at very high ionic strength is achieved. However, the modified parameters for the extended molality range cause a significant loss of accuracy at lower molalities. Because an upper ionic strength limit of about (15 to 18) mol·kg^{-1} is sufficient for the purpose of the present work, we decided to use the model parameters for $NaCH_3COO$ (aq) listed in Table 3 without modification.

In a previous study,[1] the same values for α_1 and α_2 were also successfully used for the representation of the osmotic coefficients in aqueous NaCl at 298.15 K to high supersaturation; thus, these values for α_1 and α_2 were also adopted in the present work. The determination of the coefficients of eq 13 for NaCl (aq) was largely based on the equation of Archer,[24] which accurately represents the thermodynamic properties of NaCl (aq) to the saturation molalities. The equation includes an ionic strength dependence of the third virial coefficient to improve the representation of the experimental data essentially to within their respective uncertainties. The equation was used to generate values of osmotic and activity coefficients from dilute solution to saturation and from 250 K to 383 K that were combined with data obtained from water activity measurements for supersaturated NaCl solutions at 298.15 K.[25] Particular

Table 5. Sources of Data for the System NaCl + $NaCH_3COO$ + H_2O

	T	I				
type[a]	K	$(mol \cdot kg^{-1})$	N[b]	σ_{est}[c]	σ_{fit}[d]	reference
ϕ(vp)	298.15	0.25−3.4	60 (60)	0.01	0.005	32
ϕ(iso)	298.15	1.9−3.1	6 (6)	0.003	0.004	33
$\ln \gamma_{NaCl}$	298.15	1−5	10 (15)	0.01	0.004	34
$\ln \gamma_{NaCl}$	298.15	0.1−3.5	45 (45)	0.005	0.002	35
$\ln \gamma_{NaCl}$	298.15−318.15	0.5−3	228 (228)	0.005	0.001	36
$\ln K$	278.15−323.15	5.3−11.5	24 (24)	0.05	0.05	this work

[a] Fitted quantity and experimental technique (iso, isopiestic; vp, vapor pressure osmometer). [b]Number of experimental data used in fit (total number of observations in brackets). [c]Assigned standard error. [d]Standard error of fit.

Table 6. Coefficients in Equation 13 for the Temperature Dependence of the Ternary Interaction Parameters θ and ψ

	θ	ψ
q_1	−9.35E −03	−3.56E −04
q_2		
q_3	4.04E −02	

emphasis was placed on a reasonable behavior of the model equations to concentrations as high as possible, that is, to avoid unrealistic extrema in the calculated values of the water activity and the activity of the solute. The fitting constants listed in Table 3 yield plausible values of the osmotic and activity coefficients to about 15 $mol \cdot kg^{-1}$, and the root-mean-square errors compared to the values calculated with Archer's equation are $\Delta\phi = 0.002$ and $\Delta \ln \gamma = 0.004$.

There is a huge database of excellent solubilities for both NaCl and $NaCl \cdot 2H_2O$ that could be used for the calculations of the solubility products for these salts. The parameters of eq 13 for NaCl and $NaCl \cdot 2H_2O$ listed in Table 4 were determined using a consistent set of tabulated solubilities. The use of these parameters yields an excellent representation of the experimental data. The invariant point $NaCl \cdot 2H_2O$ + solution + ice is calculated at 252.17 K and $m = 5.16$ $mol \cdot kg^{-1}$, which is also in excellent agreement with both the available experimental data[26−31] and the position of the invariant point calculated by Archer[24] (252.15 K, $m = 5.14$ $mol \cdot kg^{-1}$). Agreement to within the scatter in the experimental data[26−29] is also obtained for the position of the second invariant equilibrium NaCl + $NaCl \cdot 2H_2O$ + solution. Through the use of the present model, the equilibrium is calculated at 273.31 K and $m = 6.10$ $mol \cdot kg^{-1}$, while Archer reported 273.28 K and $m = 6.10$ $mol \cdot kg^{-1}$.

Mixing Parameters. The sources of data for the ternary system are listed in Table 5 and include isopiestic data at 298.15 K,[32,33] activity coefficients of NaCl in the range from 298.15 K to 318.15 K obtained using ion selective electrodes,[34−36] and the solubility measurements of the present work. Stenius[32] measured the water activity of aqueous $NaCH_3COO$ with a vapor pressure osmometer and NaCl standard solutions. Jones and Prue[33] used the isopiestic technique with NaCl reference solutions. In both cases, osmotic coefficients of the mixed solutions were calculated using osmotic coefficients for the NaCl solutions from Archer.[24] The activity coefficients of NaCl determined by Lanier,[34] Manohar and Ananthaswamy,[36] and Esteso et al.[35] were used as reported. However, five observations of Lanier were rejected because of their high degree of scatter. Apart from the solubility measurements of the present work, there was only one additional value of Wu and Yang[37] reported in Gmelin.[38] This observation was also zero-weighted because it lacks consistency with the remaining data.

The coefficients in eq 13 for the temperature dependence of the ternary interaction parameters θ and ψ were determined in a simultaneous least-squares fit to the experimental data. To properly weight the different types of data in the least-squares treatment, estimated standard errors listed in Table 5 were used. Error estimates are based on the reported experimental errors, the internal consistency and scatter of each data set, and the compatibility with the remaining data sets. The parameters obtained from the fit are listed in Table 6. Values of θ and ψ

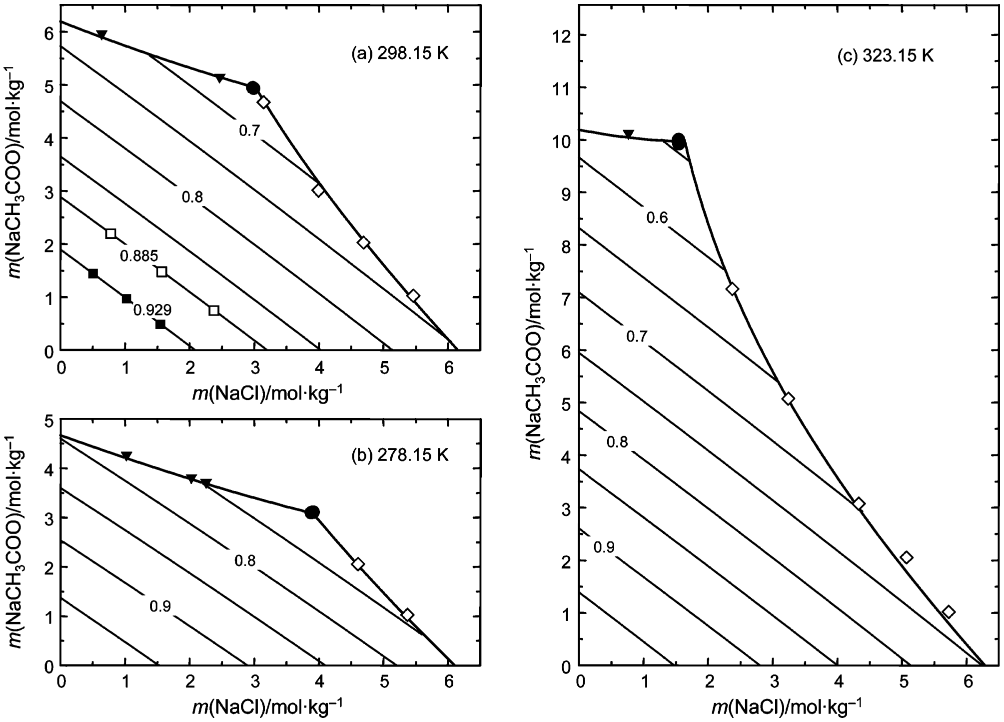

Figure 4. Solubilities and water activities in the system $NaCH_3COO$ + NaCl + H_2O at (a) 298.15 K, (b) 278.15 K, and (c) 323.15 K. Symbols represent experimental data and have the following meanings: ▲, solutions saturated with $NaCH_3COO \cdot 3H_2O$; ◇, solutions saturated with NaCl; ●, solutions saturated with $NaCH_3COO \cdot 3H_2O$ and NaCl; and ■,□, isopiestic vapor pressure data of Jones and Prue.[33] Contours represent lines of constant water activity.

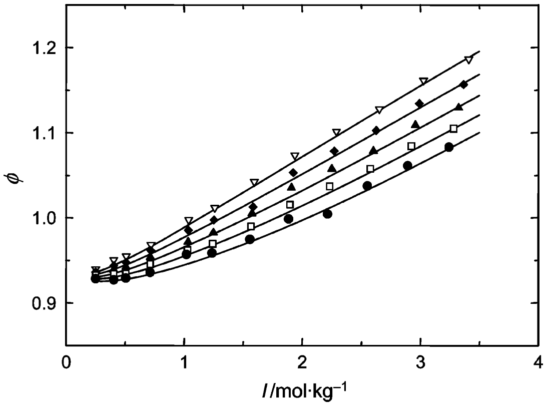

Figure 5. Osmotic coefficients ϕ in aqueous $NaCH_3COO-NaCl$ mixtures at 298.15 K plotted against ionic strength. Symbols represent experimental data of Stenius[32] at constant $NaCH_3COO$ mole fractions of: ●, $y = 0.1667$; □, $y = 0.3333$; ▲, $y = 0.5000$; ◆, $y = 0.6667$; and ▽, $y = 0.8333$.

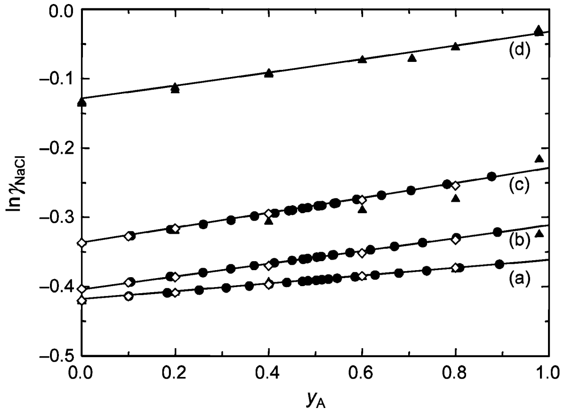

Figure 6. Activity coefficients $\ln \gamma_{NaCl}$ in aqueous $NaCH_3COO-NaCl$ mixtures at 298.15 K plotted against the mole fraction y_A of $NaCH_3COO$ at total molalities of (a) 1 mol·kg^{-1}, (b) 2 mol·kg^{-1}, (c) 3 mol·kg^{-1}, and (d) 5 mol·kg^{-1}. Symbols represent experimental data of: ●, Manohar and Ananthaswamy;[36] ◇, Esteso et al.;[35] and ▲, Lanier.[34]

and the contributions of the corresponding terms in eqs 9−11 are small. Nonetheless, their inclusion provides a significant improvement of the model at higher ionic strength, that is, for the calculation of solubilities. As indicated by the standard errors of the fit (see Table 5), the model represents the experimental data to within the stated experimental uncertainty.

The measurements are compared with values calculated using the fitted model in Figures 4 to 6. There is very good agreement for the solubility data (Figure 4). The model also provides an accurate representation of the isopiestic measurements of Jones and Prue[33] carried out at constant water activities of 0.9286 and 0.8852, respectively (Figure 4a). Osmotic coefficients reported by Stenius[32] are compared with the model in Figure 5. There appears to be a small systematic deviation of about 0.004 indicating an inconsistency between the osmotic coefficients and the activity data. However, considering the scatter in the experimental osmotic coefficients and the uncertainty inherent in the treatment of the binary system $NaCH_3COO$ (aq), it is concluded that the deviation does not exceed the combined uncertainties. The experimental and calculated activity coefficients of NaCl at 298.15 K in mixed solutions at selected ionic strengths are plotted in Figure 6. There is very good agreement essentially to within the uncertainty of the experimental data. Similar results were obtained for other ionic strengths and the other temperatures not shown in Figure 6.

To our knowledge, there are no experimental data available below 278 K. Because the system follows closely the isopiestic relation (see contour lines in Figure 4), we feel that extrapolation to lower temperature should be possible as the influence of the ternary interaction parameters in the system is only small. Values of the ternary parameters extrapolate smoothly into the low-temperature region, and test calculations confirm that calculated water activities and activity coefficients still follow the isopiestic relation at low temperature. Therefore, we believe that the present model can be also used to predict phase equilibria at lower temperatures. The invariant point for $NaCl{\cdot}2H_2O$ + $NaCH_3COO{\cdot}3H_2O$ + ice + solution is modeled at 247.14 K, 3.57 mol·kg^{-1} NaCl and 2.40 mol·kg^{-1} $NaCH_3COO$. The invariant point NaCl + $NaCl{\cdot}2H_2O$ + $NaCH_3COO{\cdot}3H_2O$ + solution is modeled at 268.04 K, 4.27 mol·kg^{-1} NaCl and 2.49 mol·kg^{-1} $NaCH_3COO$.

For the reasons discussed before, the extrapolation of the model to temperatures significantly higher than 323 K is more critical. Because of the problems with the binary interaction parameters for $NaCH_3COO$ (aq) mentioned before, the model failed to calculate the invariant point NaCl + $NaCH_3COO{\cdot}3H_2O$ + $NaCH_3COO$ + solution. Test calculations have shown however, that the $NaCH_3COO{\cdot}3H_2O$ is the stable solid to at least 329 K which was considered as an upper limit for solubility calculations using the present model. Hence, the $NaCH_3COO{\cdot}3H_2O-NaCH_3COO$ transition temperature is not significantly lowered by the presence of NaCl.

Conclusions

The present solubility measurements are consistent with available measurements of osmotic coefficients and activity coefficients in $Na^+-CH_3COO^--Cl^-$ mixtures. The Pitzer type ion interaction equations presented here provide an accurate representation of all experimental data to within the respective experimental uncertainties from 278.15 K to 323.15 K. The binary interaction parameters are valid from the freezing temperatures to about 393 K with an upper ion strength limit of about (15 to 18) mol^{-1}·kg for both $NaCH_3COO$ (aq) and NaCl (aq). The mixing parameters θ and ψ entering the ion interaction equations were found to be significant but small for the system $NaCH_3COO$ + NaCl + H_2O. A temperature independent ψ proved to be sufficient to represent the available experimental data. The equation for θ smoothly extrapolates outside the fitted temperature range from 278.15 K to 323.15 K. It is therefore concluded that extrapolation is possible to predict the solubilities and activities in mixed aqueous solutions of $NaCH_3COO$ and NaCl at temperatures outside the fitted range. At low temperatures, the solubilities do not exceed the ionic strength limit of the model allowing for accurate calculation of freezing temperatures and solubilities. At enhanced temperatures, however, the model cannot be used for solubility calculations as the ionic strength limit is exceeded.

Literature Cited

(1) Steiger, M. Crystal growth in porous materials: I. The crystallization pressure of large crystals. *J. Crystal Growth* **2005**, *282*, 455−469.

(2) FitzHugh, E.W.; Gettens, R.J. In *Science and Archaeology*; Brill, R., ed.; MIT Press: Cambridge, 1971; pp 91−102.

(3) Tennent, N. H.; Baird, T. The deterioration of mollusca collections: Identification of shell efflorescence. *Stud. Conserv.* **1985**, *30*, 73−85.

(4) Gibson, L.T.; Cooksey, B.G.; Littlejohn, D.; Linnow, K.; Steiger, M.; Tennent, N.H. The mode of formation of thecotrichite, a widespread calcium acetate nitrate chloride efflorescence. *Stud. Conserv.* **2005**, *50* 284−294.

(5) Tétreault, J. La mesure de l'acidité des produits volatils, *J. Internat. Inst. Conserv.−Can. Group* **1992**, *17*, 17−25.

(6) Linnow, K.; Halsberghe, L.; Steiger, M. Analysis of calcium acetate efflorescences formed on ceramic tiles in a museum environment. *J. Cult. Heritage* **2007**, *8*, 44−52.

(7) Königsberger, E.; Eriksson, G.; May, P. M.; Hefter, G. Comprehensive model of synthetic Bayer liquors. Part 1. Overview. *Ind. Eng. Chem. Res.* **2005**, *44*, 5804−5814.

(8) Pitzer, K.S. In *Activity Coefficients in Electrolyte Solutions*; Pitzer, K. S., ed.; CRC Press: Boca Raton, 1991; pp 75−153.

(9) Steiger, M.; Beyer, R.; Dorn, J.; Zeunert, A. In *ECOS: Environmental Control of Salts, Protection and Conservation of European Cultural Heritage Research Report*; Price, C. A., ed.; Archetype: London, 2000; pp 19−44.

(10) Beyer, R.; Steiger, M. Vapor pressure measurements and thermodynamic properties of aqueous solutions of sodium acetate. *J. Chem. Thermodyn.* **2002**, *34*, 1057−1071.

(11) Linnow, K.; Zeunert, A.; Steiger, M. Investigation of sodium sulfate phase transitions in a porous material using humidity and temperature controlled X-ray diffraction. *Anal. Chem.* **2006**, *78*, 4683−4689.

(12) Archer, D. G.; Wang, P. The dielectric constant of water and Debye-Hückel limiting law slopes. *J. Phys. Chem. Ref. Data* **1990**, *19*, 371−411.

(13) Pitzer, K. S.; Mayorga, G. Thermodynamics of electrolytes. III. Activity and osmotic coefficients for 2−2 electrolytes. *J. Solution Chem.* **1974**, *3*, 539−546.

(14) Filippov, V. K.; Barkov, D. S.; Fedorov, Y. A. Application of the Pitzer equations to the solubility of ternary aqueous nitrate solutions at 25°. *J. Solution Chem.* **1986**, *15*, 611−619.

(15) Guthrie, F. On salt solutions and attached water. V. *Philos. Mag., Ser. 5* **1876**, *2*, 211−225.

(16) Schiavon, G. Sulla solubilità dell' acetate sodico nell' acqua e nell' alcool. *Gazz. Chim. Ital.* **1902**, *32*, 532−535.

(17) Green, W. F. The "melting point" of hydrated sodium acetate: solubility curves. *J. Phys. Chem.* **1908**, *12*, 655−660.

(18) Dunningham, A. C. An exact investigation of the three component system: sodium oxide, acetic anhydride, water. *J. Chem. Soc.* **1912**, *101*, 431−444.

(19) Morgen, R. A.; Walker, R. D. The system sodium acetate−sodium hydroxide−water. *Ind. Eng. Chem.* **1945**, *37*, 1186−1188.

(20) Bonner, O. D. Osmotic and activity coefficients of the sodium salts of formic, acetic, and propionic acids. *J. Solution Chem.* **1988**, *17*, 999−1002.

(21) Miller, W. L. Indirect analysis by means of the dilatometer: the "lower hydrate" of sodium acetate. *J. Phys. Chem.* **1908**, *12*, 649−654.

(22) McBain, J. W.; Laing, M. E.; Titley, A. F. Colloidal electrolytes: Soap solutions as a type. *J. Chem. Soc.* **1919**, *115*, 1279−1300.

(23) Scatchard, G.; Prentiss, S. S. The freezing points of aqueous solutions. VI. Potassium, sodium, and lithium formates and acetates. *J. Am. Chem. Soc.* **1934**, *56*, 807−811.

(24) Archer, D. G. Thermodynamic properties of NaCl + H_2O system. II. Thermodynamic properties of NaCl (aq), $NaCl\cdot 2H_2O$ (cr), and phase equilibria. *J. Phys. Chem. Ref. Data* **1992,** *21*, 793−821.

(25) Tang, I. N. Thermodynamic and optical properties of mixed-salt aerosols of atmospheric importance. *J. Geophys. Res.* **1997**, *102*, 1883−1893.

(26) Chrétien, A. Étude du système quaternaire. Eau, nitrate de sodium, chlorure de sodium, sulfate de sodium. *Ann. Chim.* **1929**, *12*, 127−155.

(27) Foote, H. W.; Schairer, J. F. The system Na_2SO_4−NaF−NaCl−H_2O. I. The ternary systems with water and two salts. *J. Am. Chem. Soc.* **1930**, *52*, 4202−4209.

(28) Cornec, E.; Krombach, H. Équilibres entre le chlorure de potassium, le chlorure de sodium et l'eau depuis −23° jusqu'a +190°. *Ann. Chim.* **1932**, *18*, 5−31.

(29) Akopov, E. K. Solubility polytherm of ternary system LiCl−NaCl−H_2O. *J. Appl. Chem. U.S.S.R.* **1963**, *36*, 1859−1862.

(30) Potter, R. W.; Clynne, M. A.; Brown, D. L. Freezing-point depression of aqueous sodium chloride solutions. *Econ. Geol.* **1978**, *73*, 284−285.

(31) Hall, D. L.; Sterner, S. M.; Bodnar, R. J. Freezing point depression of NaCl−KCl−H_2O solutions. *Econ. Geol.* **1988**, *83*, 197−202.

(32) Stenius, P. Association equilibria and micelle formation of fatty acid sodium salts. II. An investigation of straight-chain salts vapour pressure osmometry. *Acta Chem. Scand.* **1973**, *27*, 3435−3451.

(33) Jones, R. A.; Prue, J. E. Excess Gibbs energies of aqueous mixtures of sodium chloride, potassium chloride, sodium acetate, and potassium acetate at 25°C. *J. Solution Chem.* **1974**, *3*, 585−592.

(34) Lanier, R. D. Activity coefficients of sodium chloride in aqueous three-component solutions by cation-sensitive glass electrodes. *J. Phys. Chem.* **1965**, *69*, 3992−3998.

(35) Esteso, M. A.; Hernández-Luis, F. F.; Fernández-Mérida, L.; Gonzaléz-Diaz, O. M. Activity coefficients in mixed-electrolyte solutions at 25°C: NaCl + Na-Acetate + H_2O and NaCl + Na-Propionate + H_2O systems. *J. Chem. Res., Miniprint* **1990**, 1855−1877.

(36) Manohar, S.; Ananthaswamy, J. Activity coefficients of NaCl−NaOAc−H_2O at 25, 35, and 45 °C. *Can. J. Chem.* **1991**, *69*, 111−115.

(37) Wu, C.-K.; Yang, Y. Phase diagram NaCl−NaOAc−H_2O at 20 °C. *Fu-Tan Hsueh Pao Tzu Jan K'o Hsueh* **1957**, 217−224.

(38) Gmelins Handbuch der Anorganischen Chemie, Ergänzungsband 21, Natrium, Lieferung 5, Systeme mit $NaCH_3COO$, das System $NaCH_3$-COO−NaCl−H_2O, 8. Auflage, Verlag Chemie: Weinheim, Germany, 1974.

Received for review March 24, 2007. Accepted June 11, 2007. Financial support of this research by the European Commission (Grant ENV4-CT95−0135) is gratefully acknowledged.

JE7001495